ChemPhysChem

Research Article
doi.org/10.1002/cphc.202400266

Chemistry Europe
European Chemical Societies Publishing

www.chemphyschem.org

Methyl Methacrylate Copolymer with Pendant Thioxanthenone Groups as Active Layer for Resistive Memory Devices

Danila S. Odintsov,[a] Andrei A. Gismatulin,[a] Inna K. Shundrina,[a] Alexandra D. Buktoyarova,[a] Irina A. Os'kina,[a] Jens Beckmann,*[b] Ivan A. Azarov,[c] Ekaterina V. Dementeva,[d] Leonid A. Shundrin,*[a] and Vladimir A. Gritsenko[a, e]

An electro-active copolymer of methyl methacrylate and 2-((4-acroylpiperazine-1-yl)methyl)-9*H*-thioxanthene-9-one (poly(MMA-co-ThS)) was synthesized by radical polymerization. The copolymer has good solubility in most organic solvents, thermal stability up to 282 °C and excellent ability to form thin films on silicon wafers. Poly(MMA-co-ThS) films exhibited an electrochemical and electrochromic activity resulting in the formation of long-lived radical anion states of pendant thioxanthone groups inside the film. These states exhibit optical transitions in the visible region as a broad optical absorption band, $500 < \lambda < 900$ nm ($1.38 < W_{opt}(ThS) < 2.48$ eV) with a maximum at $\lambda_{max} = 675$ nm (1.84 eV). Using temperature measurements of the current–voltage characteristics of p-Si(100)/poly(MMA-co-ThS)/Al devices, it was shown that the charge transport in the film occurs by a multiphonon mechanism, which is quantitatively described by the Nasyrov–Gritsenko model of phonon-assisted tunneling between traps. The value of the optical transition energy of the trap, determined by the Nasyrov–Gritsenko model, $W_{opt} = 1.8$ eV, is in a good agreement with $W_{opt}(ThS)$, confirming the nature of the traps as 9*H*-thioxanthen-9-one structures. The n^{++}Si(100)/poly(MMA-co-ThS)/Al memory device exhibited a memristive effect (reversible ON/OFF switching of the device) with an initial "forming" cycle followed by repetitive memory cycles characterized by bipolar switching.

Introduction

Currently, one of the most pressing problems of microelectronics is the development of a universal memory that combines high performance and an unlimited number of switching cycles of random access memory and non-volatile flash memory. One of the most promising candidates for such a memory is a memristor,[1,2] which is considered to be the fourth fundamental passive circuit element for information storage in the form of resistance.[3,4] A memristor is a device characterized by reversible switching between a high-resistance state (HRS) and a low-resistance state (LRS). This property is known as the "memristive effect".[5] Along with a number of inorganic materials used for the active media of memristors,[4,5] organic polymers are also considered to be promising materials for elaboration of memristor media due to their good film-forming ability, compatibility with metal and semiconductor platforms, structural flexibility, ease of fabrication of three-dimensional cross-bar arrays and sufficient thermal stability.[6–8] In addition, the key electrical properties of organic polymers, in particular the band gap (E_g), can be easily varied by changing the structure of the polymer chain or the chemical structures of pendant (side) groups linked with the chain.[6,7]

To understand the charge transport mechanism and memristor switching phenomena of polymer-based memory devices, a number of memory mechanisms have been proposed: charge transfer (CT),[9] conformational change,[10] traps including carbon-rich and metallic filaments,[11] ohmic conduction,[12] Schottky emission,[13] Poole–Fraenkel and thermionic emissions,[14,15] as well as the nearest neighbor hopping mechanism addressable to voltage-induced trans-to-cis isomerization.[16] Most physical models of charge transport were originally developed for inorganic semiconductors and dielectrics. Among these models, the concept of charge transport by a hopping mechanism predominates.[17–22]

To understand the physics of memristor operation and predict the power consumption of memristor memories, it is important to study the charge transport mechanisms (leakage currents) and determine the trap energies in organic polymer films.[23,25] For polymer devices, the basic charge transport

[a] *Dr. D. S. Odintsov, Dr. A. A. Gismatulin, Dr. I. K. Shundrina, Dr. A. D. Buktoyarova, Dr. I. A. Os'kina, Prof. Dr. L. A. Shundrin, Prof. Dr. V. A. Gritsenko*
Novosibirsk Institute of Organic Chemistry, Siberian Branch of the Russian Academy of Sciences, 630090 Novosibirsk, Russian Federation
E-mail: shundrin@nioch.nsc.ru

[b] *Prof. Dr. J. Beckmann*
Institute for Inorganic Chemistry and Crystallography, University of Bremen, 28359 Bremen, Germany
E-mail: j.beckmann@uni-bremen.de

[c] *Dr. I. A. Azarov*
Novosibirsk State University, 630090 Novosibirsk, Russian Federation

[d] *Dr. E. V. Dementeva*
194021 Saint Petersburg, Russian Federation

[e] *Prof. Dr. V. A. Gritsenko*
Novosibirsk State Technical University, 630073 Novosibirsk, Russian Federation

Supporting information for this article is available on the WWW under https://doi.org/10.1002/cphc.202400266

models have been summarized in ref.[26] Note that the subject of polymer-based memory switching is still controversial and strongly depends on the structure and electrical properties of the polymer used and the type of memristor structure: Metal–Insulator–Metal (MIM) or Metal–Insulator–Semiconductor (MIS).[27]

Methyl methacrylate copolymers are considered as promising materials for memristor memory, including the development of "flexible memory".[28,29] Meanwhile, 9*H*-thioxanthen-9-ones (thioxanthenones) were found to be strong electron acceptors capable of forming long-lived radical anions.[30] Thioxanthenones also found practical application in the elaboration of electroactive ambipolar polyimides with thioxanthenone-based pendant groups.[31] These polyimides featured high thermal stability, low redox potentials and a band gap of 3.15–3.42 eV.[32] Metal-insulator-semiconductor type memory devices based on these polyimides demonstrated WORM (write-once-read-many-times) nonvolatile behavior.[33] The successful use of thioxanthenones as electron acceptor units in polyimides prompted us to synthesize a methyl methacrylate copolymer containing 9H-thioxanthen-9-one pendant groups in its structure. Since the band gap of unmodified methyl methacrylate is rather high (4.5 eV)[34], the introduction of thioxanthenones can result to the appearance of traps with the low-lying boundary orbital levels "inside" E_g of methyl methacrylate. Thus, the main idea was to synthesize a copolymer (Scheme 1) with "inside" electron traps and subsequently study the electron transport mechanism in the films of poly(MMA-co-ThS) in strong electric fields in the transverse direction. The goals of our work also included establishing the trap ionization mechanism and determining the trap ionization energies. To study the trap ionization mechanism, we compared the experimental current–voltage (*IU*) characteristics of the corresponding MIS devices measured at different temperatures with various theoretical models.

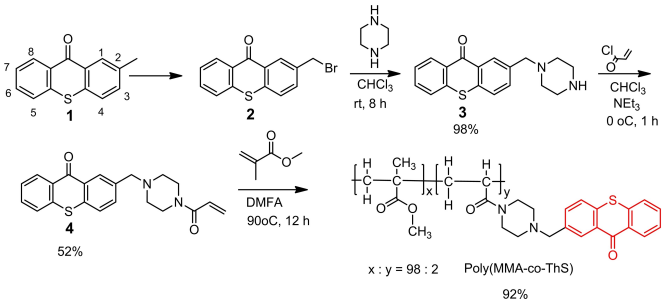

Scheme 1. Synthesis of the poly(MMA-co-ThS). The structure of the 9H-thioxanthen-9-one pendant group is shown in red.

Results and Discussion

Synthesis, Mass-Weight Characteristics, Thermal Stability and Electrochemical/Electro-optical and Cathodoluminescence Properties of Poly(MMA-co-ThS)

Poly(MMA-co-ThS) (Scheme 1) was obtained by radical copolymerization of methyl methacrylate and 2-((4-acroylpiperazine-1-yl)methyl)-9*H*-thioxanthene-9-one (**4**) in a yield of 92%. Its US-Vis-NIR spectrum in the wavelength range of $250 < \lambda < 400$ nm is determined by the presence of the 9*H*-thioxanthen-9-one pendant group in its structure (SI, Figure S7). The NMR ^{1}H spectrum of poly(MMA-co-ThS) showed the ratio of methyl methacrylate and 2-((4-acryloylpiperazin-1-yl)methyl)-9*H*-thioxanthen-9-one units in the copolymer x:y = 98:2 (SI, Figure S4). The copolymer is characterized by a high number-average molecular weight (*Mn* = 115,000) and weight-averaged molecular weight (*Mw* = 240,000) (SI, Table S1). The corresponding polydispersity index is *Mw*/*Mn* = 2.1, which is good enough for the film formation on Si wafers during the fabrication of model MIS memory devices. Poly(MMA-co-ThS) is characterized by a glass transition temperature of 127 °C. It is 40 degrees higher than the standard test temperature for resistive memory devices (85 °C). Thermogravimetry of poly(MMA-co-ThS) in inert and oxidative atmosphere showed its high thermal stability. The temperatures of 3% mass loss, T3%, are 282 °C and 297 °C, respectively (Figure 1a, SI, Table S1).

Poly(MMA-co-ThS) is well soluble in a variety of organic solvents, including those used in electrochemistry. Therefore, cyclic voltammograms (CV) of poly(MMA-co-ThS) were measured in its solution (~1%) in MeCN. The CVs of poly(MMA-co-ThS) in the potential range $2.0 > E > -2.0$ V (vs SCE) showed a

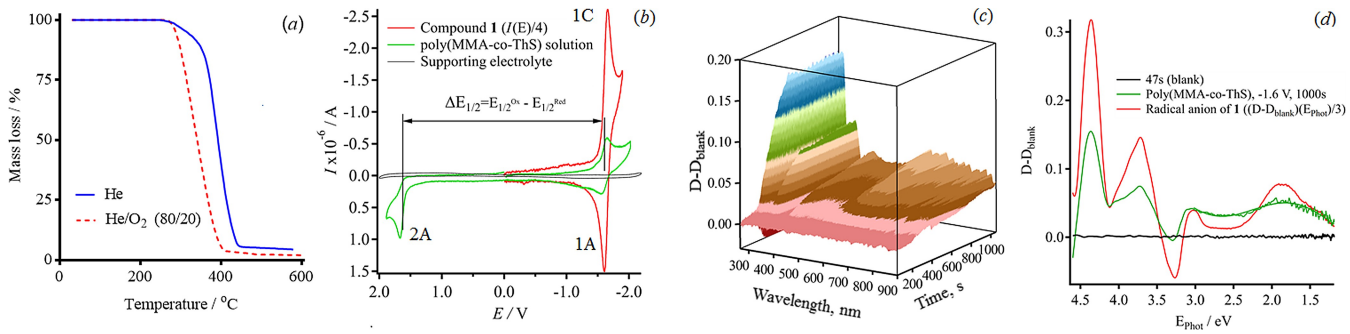

Figure 1. (*a*) TG curves of poly(MMA-co-ThS) in helium and helium/oxygen atmosphere, (*b*) cyclic voltammogram of poly(MMA-co-ThS) solution (~1%) in MeCN (green curve) together with the CV of compound **1** (red curve, $0.0 > E > -2.0$ V, CV current divided by 4, data from ref. [38]), (*c*) spectroelectrochemical surface of poly(MMA-co-ThS) solution obtained by potentiostatic electrolysis at the potential of −1.6 V, (*d*) differential optical absorption spectra: poly(MMA-co-ThS) obtained after 1000 s of electrolysis (green curve), compound **1** (red curve, data from ref. [38].)

Table 1. Reduction/oxidation peak[a] and half-wave ($E_{1/2}^{red/ox}$) potentials (V), difference in peak potentials ($\Delta E_p = E_p^{1C} - E_p^{1A}$, V), the corresponding peak currents ($I_p^{peak\ number}$) (μA), boundary orbital (LUMO/HOMO) energies (eV), and the photon energies in the maxima of optical absorption spectra (E_{phot}, eV) in neutral and electrochemically reduced[b] poly(MMA-co-ThS) in MeCN.

Reduction					Oxidation			ε_{LUMO}	ε_{HOMO}	$\Delta\varepsilon^c$	Neutral		Reduced
E_p^{1C}	E_p^{1A}	$E_{1/2}^{red}$	ΔE_p	I^{1C}/I^{1A}	E_p^{2A}	$E_{1/2}^{ox}$	I^{2A}				$E_{phot\ (on)}$	E_{phot}	E_{phot}[b]
−1.64	−1.58	−1.61	0.06	0.42/0.38	1.67	1.62[f]	0.84	−2.72	−5.95[c]	3.23[c]	3.06	4.81	4.31
									−5.78[d]	3.06[d]		4.29	3.66
												4.11	3.00
												3.25	1.84[e]

[a] Peak and $E_{1/2}$ potentials are quoted with the reference to a saturated calomel electrode (SCE). [b] Obtained in spectroelectrochemical experiment. [c] The difference $\Delta\varepsilon = |\varepsilon_{LUMO} - \varepsilon_{HOMO}|$ according to cyclic voltammetry data. [d] Calculated from optical spectrum using onset photon energy ($E_{phot\ (on)}$) (SI, Figure S7) as described in ref. [31] [e] Since optical absorption in visible region is observed as a broad absorption band, the maximum determination accuracy is ±0.04 eV. [f] Approximate value derived from data on the ECO mechanism of **1** from ref. [37].

one-electron reductive reversible CV-wave (Figure 1b, peaks 1 C, 1 A, $\Delta E_p = 0.06$ V, $I^{1C}/I^{1A} = 1.1$) associated with the formation of long-lived radical anion states of the pendant 9*H*-thioxanthen-9-one groups. The potentials of peaks 1 C, 1 A and the corresponding $E_{1/2}$ potential (Table 1) are in good agreement with the corresponding potentials observed for the ECR of 2-methyl-9*H*-thioxanthen-9-one (compound **1**, Scheme 1, CV of **1** is shown in Figure 1b), which was the precursor of the pendant groups. Electrochemical oxidation (ECO) of poly(MMA-co-ThS) was found to be irreversible (Figure 1b, peak 2 A) and at least two-electron ($I^{2A}/I^{1C} = 2.0$, Table 1).

Since poly(methyl methacrylate) itself does not show electrochemical activity over the full available range of potentials in MeCN, the electrochemical redox activity of poly(MMA-co-ThS) is associated with the pendant groups. The reversibility of the ECR indicates that the 9*H*-thioxanthen-9-one pendant groups can play the role of effective electron traps.

Potentiostatic electrolysis of compound **1** and poly(MMA-co-ThS) solutions in MeCN at a potential of −1.7 V allowed us to observe the EPR spectra of the radical anion $[\mathbf{1}]^{\bullet-}$ (Figure 2a and b) and anion-radical states of the pendant groups of the copolymer (Figure 2c and d). The hyperfine coupling constants (HFCC) of $[\mathbf{1}]^{\bullet-}$ are very close to those described previously.[37] The SOMO of $[\mathbf{1}]^{\bullet-}$ is localized throughout the thioxhanthenone fragment, and $[\mathbf{1}]^{\bullet-}$ is of the π-type of radicals.[37]

The EPR spectrum of electrochemically reduced poly(MMA-co-ThS) is characterized by HFCC values close to $[\mathbf{1}]^{\bullet-}$ and much broader lines (Figure 2c and d), resulting in a poor resolution of the spectrum. The latter is due to a more difficult mobility of the pendant groups bound to the copolymer chain compared to "free" $[\mathbf{1}]^{\bullet-}$ in solution. The observed EPR spectra demonstrated the reversibility of the electron transfer to the pendant groups of the copolymer, as well as the long-lived nature of the radical anion states of the pendant groups.

This fact is also confirmed by spectroelectrochemical studies of poly(MMA-co-ThS) solution in MeCN. Potentiostatic electrolysis of the solution at the potential corresponding to the reversible ECR of the poly(MMA-co-ThS) (−1.6 V vs Ag/AgCl) leads to the appearance of positive optical absorption bands in the entire wavelength range (Table 1), except for narrow regions around the long-wavelength absorption maxima at

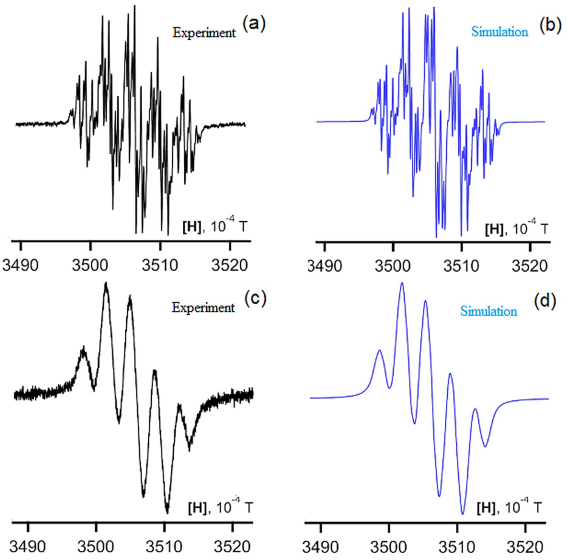

Figure 2. EPR spectral (left, black) and their simulation (right, blue) of the reduced solutions in MeCN: **1** (1.17 mM) (a,b), poly(MMA-co-ThS)(~1 %) in MeCN (c,d). Optimized ^{1}H HFCC and linewidths (LW, mT) are: $[1]^{\bullet<-M>}$: $a_1 = 0.332$, $a_2(CH_3) = 0.093$, $a_3 = 0.374$, $a_4 = 0.039$, $a_5 = 0.041$, $a_6 = 0.367$, $a_7 = 0.090$, $a_8 = 0.326$, LW = 0.019); poly(MMA-co-ThS): $a_1 = 0.332$, $a_2(CH_2) - = 0.067$, $a_3 = 0.421$, $a_4 = 0.035$, $a_5 = 0.039$, $a_6 = 0.308$, $a_7 = 0.090$, $a_8 = 0.326$, LW = 0.085). Numbering of ^{1}H nuclei is shown in Scheme 1 (Compound **1**).

385 nm (Figure 1c and d). A monotonic formation of a broad absorption band in the visible region $2.48 < E_{phot} < 1.38$ eV ($E_{phot(max)} = 1.84$ eV) with a shoulder in the near-IR region is observed (Figure 1c and d). The optical absorption spectrum (OAS) of poly(MMA-co-ThS) observed under potentiostatic electrolysis is consistent with the OAS of the 2-methyl-9*H*-thioxanthen-9-one radical anion (Figure 1d, red spectrum) described previously.[38]

The radical anion states of the pendant groups in poly(MMA-co-ThS) resulting from the one-electron capture lead to a noticeable shift of the optical absorption band maxima (Table 1) to longer wavelengths compared to the neutral states of the pendant groups. For the charged states, optical absorption is also detected in the visible wavelength region. Electrochemical and optical data showed that the difference in the LUMO/HOMO energies of the pendant groups is less than

the band gap of pure poly(methyl methacrylate).[34] This allows us to consider the thioxanthenone pendant groups as potential electron traps capable of participating in electron transport in poly(MMA-co-ThS) films.

Cathodoluminescence spectroscopy of the poly(MMA-co-ThS) film also confirmed the presence of deep electronic states in its band gap. The observed cathodoluminescence spectrum (SI, Figure S8) can be approximated by the sum of two Gaussian bands with peaks at 2.2 eV and 2.5 eV. These energies of the luminescence bands are smaller than the band gap of pure poly(methyl methacrylate) ($E_g = 4.5$ eV)[34] and $\Delta\varepsilon$ of poly(MMA-co-ThS) (Table 1), indicating the presence of deep localized electronic states in the band gap of the poly(MMA-co-ThS). Taking into account the ~2% content of pendant groups active to electron capture in the poly(MMA-co-ThS) structure (Scheme 1), the observed electronic states can also be attributed to thioxanthenone groups.

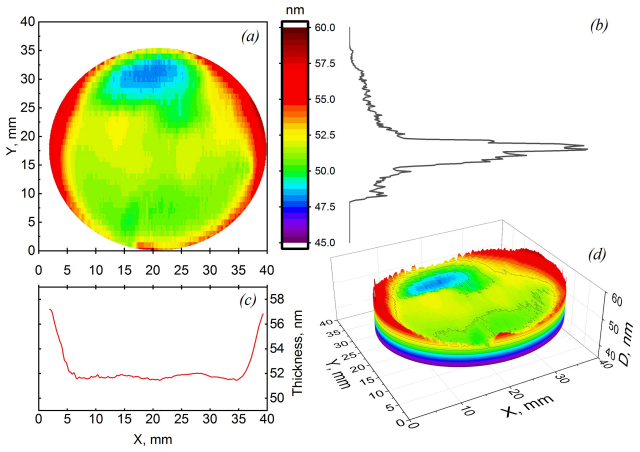

Figure 3. Results of ellipsometric mapping of n^{++}-Si(100)/poly(MMA-co-ThS): (*a*) Map of the film thickness distribution on the wafer surface, (*b*) Scale of the thickness together with the corresponding thickness statistics, (*c*) Film cross-sectional profile, (*d*) 3D image of the film distribution on the wafer surface.

MIS Memory Devices Based on Poly(MMA-co-ThS)

An example of the poly(MMA-co-ThS) thickness distribution on the n^{++}-Si(100) wafer according to spectral mapping ellipsometry applied to the entire surface of the wafer is shown in Figure 3. The map shows a characteristic radial distribution of the film thickness with a uniform central part and thickening at the edges. The characteristic range in the thickness distribution of the central part of the wafer is about 2 nm (Figure 3b), which corresponds to 4% of the total thickness (~52.5 nm on the average) and characterizes high thickness uniformity in the central part of the wafer.

For charge transport studies, a p-Si(100)/poly(MMA-co-ThS)/Al structure with an average film thickness of 60 nm was used. For memristor characterization, a n^{++}-Si(100) /poly(MMA-co-ThS)/Al structure with an average thickness of 52.5 nm was fabricated (Figure 3, SI, Figure S10).

Charge Transport in Poly(MMA-co-ThS) Film and its Modeling

Experimental *IU* characteristics of p-Si(100)/poly(MMA-co-ThS)/Al structure together with its modeling using different physical models are shown in Figure 4. To facilitate the theoretical consideration of charge transport, the *IU* characteristics are presented in the *jF* form where *j* is the current density and *F* is the electric field.

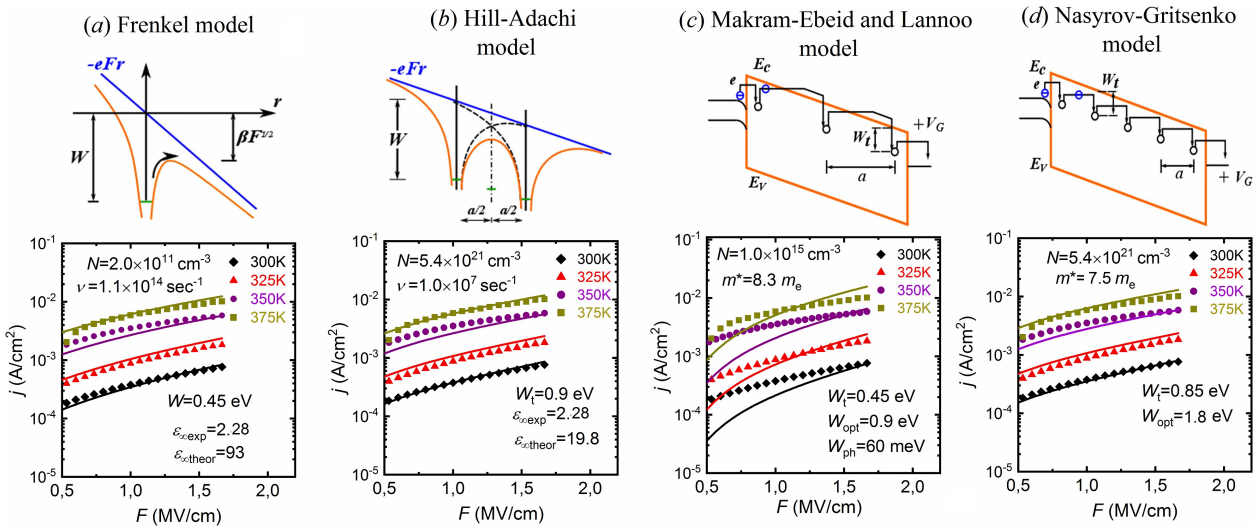

Figure 4. Experimental current–voltage characteristics (in the *jF* form) of the p-Si(100)/poly(MMA-co-ThS)/Al structure (circles) at different temperatures (indicated by color) and their comparison with: (*a*) Frenkel model, (*b*) Hill-Adachi model, (*c*) Makram-Ebeid and Lannoo model, (*d*) Nasyrov–Gritsenko model (solid curves). (*The upper images show the principles of the models, see the text below. The film thickness was 60 nm. For statistical parameters of the models and χ^2 criteria, see SI, Table S3, Figure S11*)

Frenkel Model

In the Frenkel model,[17] (Figure 4a), the current density j through a dielectric with electron traps is described by the following expression[20]:

$$j = \frac{e}{a^2}P = eN^{2/3}P \tag{1}$$

where $N = a^{-3}$ is the concentration of traps, a is the mean distance between traps, and P is the trap ionization probability described by the formula:

$$P = \nu \exp\left(-\frac{W - \left(\frac{e^3}{\pi\varepsilon_\infty\varepsilon_0}\right)^{1/2}\sqrt{F}}{kT}\right) \tag{2}$$

where $\nu = W/h$ is the attempt to escape factor, W is the trap ionization energy, h is the Planck constant, e is the electron charge, $\varepsilon_\infty = n^2$ is the high-frequency permittivity, n is the refractive index, ε_0 is the dielectric constant, F is the electric field, k is the Boltzmann constant and T is temperature.

According to the Frenkel effect, the exponential dependence of the current density on the electric field is due to a decrease in the Coulomb barrier in the electric field (Figure 4a). The trap ionization energy of 0.45 eV was determined from the temperature dependence of the current. The corresponding attempt to escape factor was found to be $\nu = 1.1\times10^{14}$ s^{-1}. The experimental value of the high-frequency dielectric constant, $\varepsilon_\infty = 93$, was determined from the slope of the *jF* curves. The high-frequency dielectric constant value determined by ellipsometry (SI) is $\varepsilon_\infty = n^2 = (1.51)^2 = 2.28$. Meanwhile, the dielectric permittivity, ε_∞, determined by modeling using the Frenkel effect, is almost forty times larger than the corresponding experimental value. Thus, the Frenkel effect does not describe the charge transport and trap ionization inside the film. In addition, the use of the Frenkel model led to an immeasurably low theoretical value of the trap concentration, $N = 2.0\cdot10^{11}$ cm^{-3} (Figure 4a), which is at least 7 orders of magnitude lower than the usual measurable trap concentration in insulators, for example, in inorganic dielectrics (10^{18}–10^{21} cm^{-3}).[17]

Hill-Adachi Model

The Hill-Adachi model considers the transition of an electron between neighboring traps at a high trap concentration, when the transition barrier between the traps is lowered due to the overlap of the Coulomb potentials,[18,19] (Figure 4b). The expression for the trap ionization probability in this model has the form:

$$P = 2\nu \exp\left(-\frac{W - \frac{e^2}{\pi\varepsilon_\infty\varepsilon_0 a}}{kT}\right)\sinh\left(\frac{eFa}{2kT}\right) \tag{3}$$

The trap concentration determined from the slope of the current–voltage characteristic curves has a reasonable value $N = 5.4\cdot10^{21}$ cm^{-3}. However, the attempt to escape factor has an abnormally small value ($\nu = 1\cdot10^{7}$ s^{-1}). Thus, the Hill-Adachi model does not describe the experimental data.

Makram-Ebeid and Lannoo Model

Multiphonon trap ionization is observed at a relatively low trap concentration (10^{18}–10^{19}) cm^{-3} when the distance between the traps is relatively large. In this case, an electron is transferred from the ground state of a deep trap to an excited state due to multiphonon absorption, and then tunnels into the conduction band.[39–41] The phenomenon of multiphonon trap ionization has been successfully described by the Makram-Ebeid and Lannoo quantum model.[42] In this model, the exact probability of multiphonon ionization of a trap at a low concentration of isolated traps is given by the following equations:

$$P = \sum \exp\left\{\frac{nW_{ph}}{2kT} - \frac{W_{opt} - W_t}{W_{ph}}\coth\frac{W_{ph}}{2kT}\right\} I_n \times \times\left(\frac{W_{opt} - W_t}{W_{ph}\sinh(W_{ph}/2kT)}\right) P_i(W_t + nW_{ph}) \tag{4}$$

$$P_i = \frac{eF}{2\sqrt{2m^*(W_t + n\omega_{ph})}}\exp\left(-\frac{4}{3}\frac{\sqrt{2m^*}}{\hbar eF}(W_t + n\omega_{ph})^{3/2}\right) \tag{5}$$

where I_n is a modified Bessel function, $P_i(W)$ is the tunneling probability through a triangular barrier of height W, W_t is the thermal ionization energy of a trap, W_{opt} is the optical ionization energy of a trap, W_{ph} is the phonon energy, m^* is the effective electron mass and k, T have their usual meanings.

An attempt to use the Makram-Ebeid and Lannoo model to simulate the experimental *jF* curves led to poor match (Figure 4c). In addition, the determined theoretical trap concentration, $N = 1.0\cdot10^{15}$ cm^{-3}, is too low to implement this model.

Nasyrov and Gritsenko Model

When the concentration of traps in a dielectric is high, the multiphonon ionization phenomenon can be successfully described by the theory developed by Nasyrov and Gritsenko (NG model).[43] In this theory, an electron is excited from the ground state of a "filled" trap to its excited state. Then, it tunnels to the excited state of a neighboring "empty" trap followed by relaxation to the ground state of that trap (Figure 5a). Note that electron tunneling occurs into the neighboring trap rather than into the conduction band, as it was postulated in the Makram-Ebeid and Lannoo theory.

The equation for the ionization probability of traps in the NG model of phonon-assisted tunneling via neighboring traps has the form:

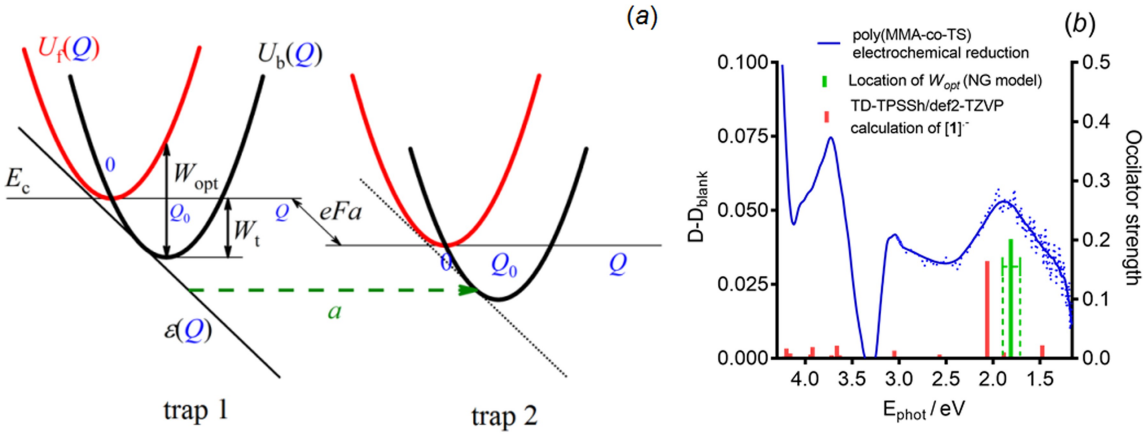

Figure 5. (*a*) Configuration diagrams of two neighboring traps in an electric field with distance *a* between the traps (down curves correspond to the ground (filled) states, upper curves correspond to excited (unoccupied) states); (*b*) differential optical absorption spectrum of poly(MMA-co-ThS) in the visible wavelength region (left axis) together with electronic transitions calculated for the radical anion of 2-methyl-9*H*-thioxanthene-9-one ($[1]^{\bullet<-M>}$) at the TD-TPSSh/def2-TZVP level of theory,[38] and the position of the W_{opt} value obtained by the NG model (bars, right axis, statistical error is shown as green dotted bars).

$$P = \frac{2\sqrt{\pi}\hbar W_t}{m^* a^2 \sqrt{2kT(W_{opt} - W_t)}} \exp\left(-\frac{W_{opt} - W_t}{kT}\right) \times \times \exp\left(-\frac{2a\sqrt{2m^* W_t}}{\hbar}\right) \sinh\left(\frac{eFa}{2kT}\right) \quad (6)$$

where P is the trap ionization probability, $\hbar$ is the reduced Planck constant, a is an average distance between traps and W_t, W_{opt}, m^*, e, F,k, T have their above meanings.

In the NG model, the trap ionization probability depends exponentially on the distance between neighboring traps, $a = N^{-1/3}$, and, thus, on the trap concentration N. So, the trap concentration N can be determined from the slope of the jF curves. The simulation with the NG model led to $N = 5.4 \cdot 10^{21}$ cm^{-3}, $W_t = 0.9$ eV, $W_{opt} = 1.8$ eV and effective mass $m^* = 7.5\ m_e$. (Figure 4d). In our opinion, the overestimated value of the electron tunneling mass is associated with high concentration of traps where the presence of space charge in the dielectric should be taken into account. This charge leads to the dependence of the local electric field on the normal coordinate in the z-direction ($F(z)$).[44] However, in this study, we used a simplified model that does not take into account the presence of space charge.

The optical ionization energy of the trap in a thin Poly(MMA-co-ThS) film, $W_{opt} = 1.8$ eV, calculated using the NG model turned out to be within the broad optical absorption band ($1.38 < W_{opt}(ThS) < 2.48$ eV) observed in the experimental optical absorption spectra of the electrochemically reduced poly(MMA-co-ThS) film (Table 1). Transitions in the visible wavelength region obtained by spectroelectrochemistry (Figure 1c and d, Figure 5b) were unambiguously interpreted as optical transitions associated with *radical anion states* of the pendant 9*H*-thioxanthen-9-one groups, which actually are the "filled" traps. TD-DFT calculations of the optical transitions of the 2-methyl-9*H*-thioxanthen-9-one radical anion, in the visible wavelength region also showed optical transition energies close to W_{opt} (Figure 5b).[38] This fact together with the observed experimental data confirms the nature of the traps in the poly(MMA-co-ThS) film as pendant groups.[45] In our opinion, this is the first example where the nature of traps was determined directly based on a comparison of the optical transition energies observed for long-lived radical anion states of pendant groups in a polymeric insulator and the optical ionization energy of traps obtained by analyzing the current–voltage characteristics of the MIS structure based on this insulator.

Memristive Effect in a n^{++}-Si(100)/Poly(MMA-co-ThS)/Al Memory Device

The experimental current–voltage (*IU*) characteristics of the model memory device based on Poly(MMA-co-ThS) film (d = 52.5 nm) showed a memristive effect (Figure 6). This memristor has an initial "forming" process, in which the device switches from an initial high-resistance state (HRS) to a low-resistance state (LRS) at a positive voltage. The LRS is maintained as the voltage sweep changes to negative values up to $U = -4.8$ V (Figure 6, curves *2, 3*). Then, when the sweep sign is reversed, the device returns back to HRS (Figure 6, curve *4*). This memory effect is repeated by cycling the voltage over the $-6.0 < U < +3.0$ V sweep range without noticeable changes in the current ratio of the HRS/LRS branches.

The charge transport mechanism in the initial HRS state before "forming switching" (Figure 6, curve *1*) at $U = -1.7$ V is well described by the NG model. To describe the charge transport in the HRS and LRS of the memristor memory cycle, a space-charge-limited current (SCLC) model[46,47] was successfully applied (SI, Figure S12).

Thus, we consider poly(MMA-co-ThS) as a promising material for potential practical use in memristor manufacturing by optimizing the composition of poly(MMA-co-ThS) (x:y ratio),

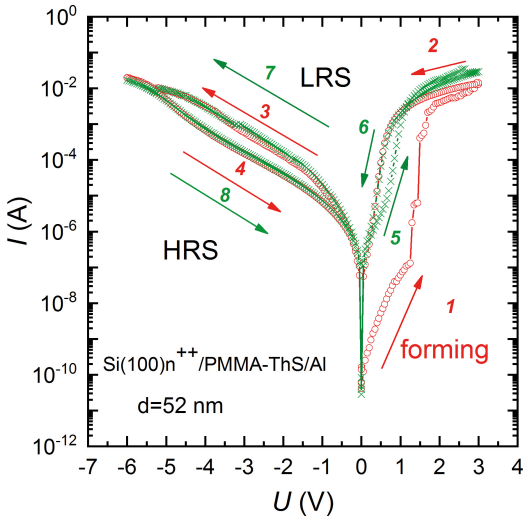

Figure 6. *IU* characteristics of n^{++}-Si(100)/Poly(MMA-co-ThS)/Al memristor with 52.5 nm insulator layer. (*Circles indicate the first cycle, Crosses indicate the second and subsequent cycles. Arrows indicate the direction and order of voltage sweep*).

the materials of the wafers, the material of the top electrodes, and the thickness of the working polymer layer. It should be noted that the described memristive effect was observed using a n^{++}-Si(100) wafer. Meanwhile, the absolute majority of the described organic polymers based memristors were fabricated using ITO- wafers, i.e. they were MIM-type structures.[6–8] So, poly(MMA-co-ThS) may be useful for the development of polymer-based memristors on silicon platforms.

Conclusions

A methyl methacrylate copolymer containing electron-withdrawing 9*H*-thioxanthen-9-one pendant groups in its structure was synthesized by radical polymerization. This co-polymer exhibited good solubility in most organic solvents, including those used in centrifugation technologies, thermal stability up to 282 °C, and fine ability to form thin films on silicon wafers. Poly(MMA-co-ThS) demonstrated electrochemical, electrochromic and cathodoluminescent activity. The electrochemical reduction of poly(MMA-co-ThS) leads to the formation of long-lived radical anion states of the pendant groups, which exhibit optical transitions in the visible region.

Using temperature measurements of the current–voltage characteristics of the p-Si(100)/poly(MMA-co-ThS)/Al structures, the charge transport in the poly(MMA-co-ThS) film and the trap ionization mechanism were studied by comparative simulation of the current–voltage curves with a number of physical models. It was shown that the charge transport occurred via a multiphonon mechanism quantitatively described by the Nasyrov–Gritsenko model of phonon-assisted tunneling between traps. The value of the optical trap energy determined by the Nasyrov–Gritsenko model is in good agreement with the experimental optical transition energy of the radical anion states of the pendant groups, confirming the nature of the traps as 9*H*-thioxanthen-9-one structures. For the first time, the nature of the traps has been identified using a combination of spectroelectrochemical and electrophysical measurements.

n^{++}-Si(100)/poly(MMA-co-ThS)/Al memory devices exhibit a memristive effect with an initial "forming" cycle followed by repetitive memory cycles characterized by bipolar switching. The charge transport mechanism in the HRS and LRS of the poly(MMA-co-ThS)-based memristor is well described by the space-charge-limited current model when the trap distribution is assumed to be exponential.

We believe that poly(MMA-co-ThS) will find its practical application in polymer-based memristor technologies, since the ratio of the main fragments of the polymer chain and the pendant electron-withdrawing groups can be easily optimized according to the specific tasks of memristor organic electronics.

Experimental Section

General

The ^{1}H, ^{13}C, NMR spectra were measured with Bruker AV-400, AV-600 spectrometers at frequencies of 400 (600) and 150.9, MHz, respectively; with standard TMS. The molecular weight characteristics of poly(MMA-co-ThS) were determined by gel permeation chromatography (GPC) using an Agilent LC-1200 chromatograph (Agilent Technologies, USA) equipped with a PL 1110–6500-gel 5 μm Mixed-C column. Tetrahydrofuran was used as the eluent at a flow rate of 1 mL/min at 40 °C. Polystyrene standards from Waters (USA) were used to calibrate the chromatograph. Thermogravimetric analysis (TGA) and differential scanning calorimetry (DSC) were performed using a STA 409 synchronous thermal analyzer (Netzsch, Germany) at the heating rate of 10 °C/min. The glass transition temperature (T_g) was determined from the DSC curves as the center of the transition step in the second heating cycle in a helium flow. The cathodoluminescence (CL) properties of poly(MMA-co-ThS) films and the dynamics of the electron beam absorbed current were studied using a CAMEBAX electron probe microanalyzer (Cameca, France) equipped with an optical spectrometer of original design for recording cathodoluminescence spectra.[36]

Synthesis

General

Poly(MMA-co-ThS) was obtained starting from 2-methyl-9*H*-thioxantane-9-one **1**. 2-Methyl-9*H*-thioxanthen-9-one **1** was synthesized and successively converted into the 2-bromomethyl-9*H*-thioxanthen-9-one **2** according to reported procedures.[30] 2-Bromomethyl-9*H*-thioxanthen-9-one **2** was reacted with piperazine in chloroform to give 2-(piperazin-1-ylmethyl)-9*H*-thioxanthen-9-one **3**. 2-((4-Acryloylpiperazin-1-yl)methyl)-9*H*-thioxanthen-9-one **4** was prepared by the treatment of 2-(piperazin-1-ylmethyl)-9*H*-thioxanthen-9-one **3** with acryloyl chloride in dichloromethane. Poly(MMA-co-ThS)) was isolated in the reaction of 2-((4-acryloylpiperazin-1-yl)methyl)-9*H*-thioxanthen-9-one **4** with methyl methacrylate in dimethylformamide (Scheme 1).

Compound 3

A solution of 0.305 g (0.001 mol) of 2-bromomethyl-9*H*-thioxanthen-9-one **2** in 30 mL of chloroform was added drop by drop to the

solution of 0.258 g (0.003 mol) of piperazine in 30 mL of chloroform for 0.5 h. The reaction mixture was stirred for 8 h at room temperature, washed with water (3×20 mL), the organic layer was dried with magnesium sulphate, the solvent was evaporated in vacuum using a rotary evaporator. The yield of compound **3** was 0.3 g, 98%. The synthesized compound **3** was used at the next stage without purification. ^{1}H NMR spectrum, δ, ppm, *J*, Hz: 8.58 (d, $J=7.9$, $1H_{Ar}$), 8.47 (s, $1H_{Ar}$), 7.62 (d, $J=7.9$, $1H_{Ar}$), 7.59–7.48 (m, $3H_{Ar}$), 7.44 (m, $1H_{Ar}$), 3.59 (s, 2H, CH_2), 3.45 (m broad., 1H, CH_2–NH), 2.92 (m, 3H, CH_2–NH), 2.48 (m, 4H, CH_2–N).

Compound 4

Dichloromethane 20 mL, 0.21 mL (0.0015 mol) of triethylamine, 0.31 g (0.001 mol) of 2-(piperazin-1-ylmethyl)-9*H*-thioxanthen-9-one **3** were charged into a three-neck flask 100 mL in volume, equipped with a mechanical mixer, thermometer and a back-pressure dropping funnel, and the mixture was cooled to 0 °C. Under mixing at a temperature of 0–5 °C, a solution of 0.12 mL (0.0015 mol) of acryloyl chloride in 20 mL of dichloromethane was added drop by drop for 0.5 h. The temperature of reaction mixture was then let to rise to the room temperature, mixing was carried out for 1 h, then the mixture was washed with water to achieve the neutral medium, the organic layer was dried with magnesium sulphate, the solvent was evaporated in vacuum using the rotary evaporator. The residue was chromatographed on silica gel. The eluent was $CHCl_3/C_2H_5OH$ (C_2H_5OH gradient from 0 to 5%). The solvents were evaporated in vacuum using a rotary evaporator. The yield of compound **4** was 0.3 g, 52%, yellow powder, m.p. 90 °C. IR spectrum, ν, cm^{-1}: 1641 (C=O), 1608 (C=C), 1591 (C=O). ^{1}H NMR spectrum, δ, ppm, *J*, Hz: 8.61 (d, $1H_{Ar}$, $J=7.9$ Hz), 8.50 (s, $1H_{Ar}$), 7.65 (d, $1H_{Ar}$, $J=7.9$ Hz), 7.62–7.52 (m, $3H_{Ar}$), 7.47 (m, $1H_{Ar}$), 6.52 (d.d, 1H, C<u>H</u>=CH_2, $J=17.0$, 10.0), 6.26 (d.d, 1H, CH=C<u>H</u>$_2$, $J=17.0$, 2.0), 5.66 (d.d, 1H, CH=C<u>H</u>$_2$, $J=10.0$, 2.0), 3.69 (m, 2H, CH_2–N), 3.63 (s, 2H, CH_2), 3.54 (m, 2H, CH_2–N), 2.46 (m, 4H, $2CH_2$–N). ^{13}C NMR spectrum, δ, ppm: 179.65, 165.08, 136.97, 136.13, 135.96, 132.93, 132.06, 129.65, 129.60, 128.94, 128.72, 127.60, 127.24, 126.09, 125.99, 125.80, 61.91, 52.90, 52.46, 45.52, 41.69. Mass spectrum: 364.1234 [M+]. $C_{21}H_{20}O_2N_2S$. M = 364.1240.

Poly(MMA-co-ThS)

Methyl methacrylate (0.971 g, 9.7 mmol), compound **4** (0.109 g, 0.3 mmol) and lauryl peroxide (0.0398 g, 0.1 mmol) were dissolved in 2 mL of dimethylformamide. To remove oxygen, the solution was bubbled with gaseous argon for 0.5 h. After that, the reaction mixture was mixed for 12 h at 90 °C. When the reaction was completed, the synthesized polymer was precipitated in methanol (25 mL), and the resulting dispersion was centrifuged to from the precipitate. The precipitate was twice re-precipitated by dissolving the polymer in chloroform, and dried in a vacuum furnace at 60 °C. The yield of Poly(MMA-co-ThS) was 92%. ^{1}H NMR spectrum, δ, ppm,: 8.59 (m, H_{Ar}), 8.50 (m, H_{Ar}), 7.66–7.51 (m, H_{Ar}), 7.46 (m, H_{Ar}), 3.68 (m, CH_2, CH, superposition of signals), 3.56 (m, OCH_3, superposition of signals), 3.44 (m, CH_2, CH, superposition of signals), 2.59–2.34 (m, CH_2, CH, superposition of signals), 2.05–1.97 (m, CH_2, CH, superposition of signals), 1.97–1.8 (m, CH_2, CH, superposition of signals), 1.77 (m, CH_2, superposition of signals), 1.47–1.34 (s, CH_3, superposition of signals), 1.27–1.14 (s, CH_3, superposition of signals), 0.98 (s, CH_3, superposition of signals), 0.81 (s, CH_3, superposition of signals). ^{13}C NMR spectrum, δ, ppm: 179.90, 178.36, 178.06, 177.79, 177.10, 176.91, 176.14, 137.22, 136.81, 136.71, 136.11, 133.19, 132.30, 132.28, 129.87, 129.23, 128.99, 126.34, 126.23, 126.06, 126.05, 62.06, 59.65, 58.33, 54.49, 54.16, 52.69, 51.75, 45.56, 44.95, 44.52, 38.16, 31.91, 31.25, 29.66, 19.02, 18.64, 16.45.

CV, EPR and UV-VIS-NIR Spectroelectrochemistry

The CV measurements for **1** and poly(MMA-co-ThS) (1.17 mM and ~1% solutions in MeCN) were performed at 295 K in an argon atmosphere using a standard electrochemical glass cell with a solution volume of 5 mL connected to a PG 310 USB potentiostat (HEKA Elektronik, Germany) with a three-electrode circuit. A stationary Pt disc electrode was used as a working electrode. The working electrode area, *A*, was 0.0122 cm^2 (calibrated using ferrocene as a standard). A Pt helix was used as an auxiliary electrode. Peak potentials were quoted with a reference to a saturated calomel electrode (SCE). A bridge with 0.1 M of supporting electrolyte in MeCN was used to connect the cell and SCE. The measurements were performed at 295 K. A 0.1 M solution of Et_4NClO_4 in MeCN was used as a supporting electrolyte in all CV experiments. All CV curves were measured using a triangular potential sweep.

The EPR spectra of radical anion 1 and electrochemically reduced poly(MMA-co-ThS) were obtained using potentiostatic electrolysis with a widely used electrochemical cell for EPR measurements equipped with a Pt working electrode placed into the EPR cavity. An ELEXSYS E-540 spectrometer (X-band, MW frequency ~9.87 GHz, MW power 20 mW, modulation frequency 100 kHz, and modulation amplitude 0.007 mT) equipped with a high-Q cylindrical resonator ER4119HS was used to record the EPR spectra. Potentiostatic electrolysis of compound **1** and poly(MMA-co-ThS) at the potentials of the first reduction peak was carried out under anaerobic conditions (oxygen was removed by well-known "Freeze-Pump-Thaw Degassing" method with a vacuum line) at 295 K. A potentiostat "Ellins P-20X" (Russia) was used for electrolysis. The electrolysis was performed in MeCN with 0.1 M solution of Et_4NClO_4 used as the supporting electrolyte. Simulations of the experimental EPR spectra were accomplished with the *Winsim 2002* program.[48] The *Simplex* algorithm was used for optimization of HFCC and line widths.

3D UV-VIS-NIR spectroelectrochemical measurements of poly(MMA-co-ThS) solution (5 mg of poly(MMA-co-ThS) in 6 mL of MeCN) were performed at 295 K. A TSC spectroelectrochemical cell (RHD instruments, Germany) with an optical path of 0.16 cm was used. A platinum mesh electrode was employed as a working electrode, and an Ag/AgCl pseudo reference electrode was used as a reference electrode. The cell was connected to a PGSTAT 101 potentiostat (Metrohm Autolab) via a three-electrode circuit and simultaneously to a UV-VIS-NIR spectrophotometer (AvaSpec-ULS2048CL-EVO Avantes) via a fiber-optic line. The UV-VIS-NIR spectra were recorded in a differential form ($D(\lambda) - D_{blank}(\lambda)$), where $D(\lambda)$ is the optical density at wavelength λ recorded during reduction, $D_{blank}(\lambda)$ is the spectrum of a neutral form of the poly(MMA-co-ThS) solution in MeCN recorded before the electrochemical reduction. All cell manipulations were performed under nitrogen in a glove box. The potentiostat was synchronized with the spectrophotometer using the Nova 2.1.2 software synchronized with the AvaSoft 8.7 software. Both programs were used for simultaneous acquisition of optical and electrochemical data in a potentiostatic mode with a potential of −1.7 V (vs Ag/AgCl). Final data analysis was performed using Igor PRO 8.0 software.

MIS Device Fabrication

The poly(MMA-co-ThS) polymer films were deposited by centrifugation on p-Si (100) and n^{++}-Si (100) wafers with resistances of 10 Ohm·cm and 0.002 Ohm·cm, respectively. A spin coater "spin NXG–P1AC" (Apex Instruments, India) equipped with a special customized nozzle for spin coating in a saturated solvent vapor atmosphere was used for centrifugation (SI). Prior to deposition of

the active layer, the Si wafer was pre-treated with a 10% HF solution to remove the oxide film. A 1% solution of poly(MMA-co-ThS) in chloroform was applied to the planar side of the silicon wafer placed in the hermetically sealed nozzle with the internal atmosphere saturated with chloroform vapor. The wafer was then centrifuged at an appropriate angular speed and time until the required poly(MMA-co-ThS) film thickness was obtained. After centrifugation, the wafer was kept in the closed nozzle for 2 min. Then, the nozzle was opened and the wafer with the deposited polymer layer was dried in air at room temperature for 30 min and in an oven at 120 °C for 2 h. Thickness control was performed by spectral ellipsometry. An array of top Al electrodes was obtained by thermal vacuum spraying with an "Academvac" high vacuum system (Russia) at $P = 1 \cdot 10^{-5}$ mm Hg using a shadow mask with an array of 0.707×0.707 mm square cells.

Spectral Ellipsometry and Current-Voltage Characteristics

The thickness (d) and refractive indices of poly(MMA-co-ThS) films deposited on Si wafers were studied using a spectral mapping ellipsometer "Ellips-1881 SAG" (Russia)[35] with an operating wavelength range of $250 < \lambda < 1000$ nm and a line width of 5 nm. The measurement resolution was 2 nm. The ellipsometer was equipped with a He–Ne laser ($\lambda = 632.8$ nm) and a focusing head. The sample for ellipsometric measurements was placed on the sample holder with a positioning accuracy of 5 μm. The thickness map was calculated from the measured ellipsometric spectra using a one-layer optical model (SI).

The current–voltage characteristics of MIS memory devices based on poly(MMA-co-ThS) as the active medium were measured with a Keithley 2400 semiconductor analyzer at various temperatures in a closed box without access to light. All the measurements were performed with the maximum current of 0.1 A.

Supporting Information Summary

The authors have cited additional references within the Supporting Information.[49–51].

Acknowledgements

The authors are grateful to the Russian Science Foundation (Project 22-13-00108, synthesis, device fabrication, electrophysical measurements) and the Deutsche Forschungsgemeinschaft (J.B. – project BE 3616/6-2, spectroelectrochemistry) for financial support. They are also grateful to the Multi-Access Chemical Research Center of the Siberian Branch of the Russian Academy of Sciences for instrumental facilities and also to the Center of Collective Use "VTAN" of the ATRC Department of the Novosibirsk State University for the opportunity to perform electrophysical measurements.

Conflict of Interests

The authors declare no conflict of interest.

Data Availability Statement

The data that support the findings of this study are available in the supplementary material of this article.

Keywords: Organic polymers · Spectroelectrochemistry · Pendant groups · Charge transport · Memristor

[1] D. B. Strukov, G. S. Snider, D. R. Stewart, R. S. Williams, *Nature* **2008**, *453*, 80.
[2] M. A. Zidan, J. P. Strachan, W. D. Lu, *Nat. Electr.* **2018**, *1*, 22.
[3] L. Chua, *IEEE Trans. Circuits Theor.* **1971**, *18*, 507.
[4] S. Pi, C. Li, H. Jiang, W. Xia, H. Xin, J. J. Yang, Q. Xia, *Nat. Nanotechnol.* **2019**, *14*, 35.
[5] A. Aglikov, O. Volkova, A. Bondar, I. Moskalenko, A. Novikov, E. V. Skorb, E. Smirnov, *ChemPhysChem* **2023**, *24*, e202300187.
[6] Q.-D. Ling, D.-J. Liaw, C. Zhu, D. S.-H. Chan, E.-T. Kang, K.-G. Neoh, *Prog. Polym. Sci.* **2008**, *33*, 917.
[7] W.-P. Lin, S.-J. Liu, T. Gong, Q. Zhao, W. Huang, *Adv. Mater.* **2014**, *26*, 570.
[8] A. J. J. M. van Breemen, J.-L. van der Steen, G. van Heck, R. Wang, V. Khikhlovskyi, M. Kemerink, G. H. Gelinck, *Appl. Phys. Express* **2014**, *7*, 031602.
[9] C. W. Chu, J. Ouyang, J.-H. Tseng, Y. Yang, *Adv. Mater.* **2005**, *17*, 1440.
[10] E. Y. H. Teo, Q. D. Ling, Y. Song, Y. P. Tan, W. Wang, E. T. Kang, D. S. H. Chan, C. Zhu, *Org. Electron* **2006**, *7*, 173.
[11] A. Wierschem, F.-J. Niedernostheide, A. Gorbatyuk, H.-G. Purwins, *Scanning* **1995**, *17*, 106.
[12] C. Wu, F. Li, T. Guo, T. W. Kim, *Org. Electr.* **2012**, *13*, 178.
[13] K. Kim, S. Park, S. G. Hahm, T. J. Lee, D. M. Kim, J. C. Kim, W. Kwon, Y. G. Ko, M. Ree, *J. Phys. Chem. B* **2009**, *113*, 9143.
[14] Y. Li, Y. Chu, R. Fang, S. Ding, Y. Wang, Y. Shen, A. Zheng, *Polymer* **2012**, *53*, 229.
[15] G. Tian, S. Qi, F. Chen, L. Shi, W. Hu, D. Wu, *Appl. Phys. Lett.* **2011**, *98*, 203302.
[16] D. Attianese, M. Petrosino, P. Vacca, S. Concilio, P. Iannelli, A. Rubino, S. Bellone, *IEEE Electr. Dev. Lett.* **2008**, *29*, 44.
[17] J. Frenkel, *Phys. Rev.* **1938**, *54*, 647.
[18] S. D. Ganichev, E. Ziemann, W. Prettl, I. N. Yassievich, A. A. Istratov, E. R. Weber, *Phys. Rev. B* **2000**, *61*, 10361.
[19] H. Schroeder, *J. Appl. Phys.* **2015**, *117*, 215103.
[20] V. A. Gritsenko, T. V. Perevalov, V. A. Voronkovskii, A. A. Gismatulin, V. N. Kruchinin, V. S. Aliev, V. A. Pustovarov, I. P. Prosvirin, Y. Roizin, *ACS Appl. Mater. Interfaces* **2018**, *10*, 3769.
[21] A. N. Aleshin, J. Y. Lee, S. W. Chu, S. W. Lee, B. Kim, S. J. Ahn, Y. W. Park, *Phys. Rev. B* **2004**, *69*, 214203.
[22] K. A. Nasyrov, V. A. Gritsenko, *Physics - Uspekhi* **2013**, *56*, 999.
[23] A. Hirao, H. Nishizawa, M. Sugiuchi, *Phys. Rev. Lett.* **1994**, *75*, 1787.
[24] D. H. Dunlap, P. E. Parris, V. M. Kenkre, *Phys. Rev. Lett.* **1996**, *77*, 542.
[25] S. V. Novikov, D. H. Dunlap, V. M. Kenkre, P. E. Parris, A. V. Vannikov, *Phys. Rev. Lett.* **1998**, *81*, 4472.
[26] D. Braun, *J. Polym. Sci.: Part B: Polym. Phys.* **2003**, *41*, 2622.
[27] A resistive memory device is a multilayer structure consisting of a wafer (metal or semiconductor, usually Si), an active insulator (dielectric) layer typically 5–80 nm thick, and a top metal electrode (Al, Cu, Ni, etc.). If a wafer is metallic, the memristor structure is called Metal-Insulator-Metal (MIM). If the wafer is semiconductor, the memristor structure is called Metal-Insulator-Semiconductor (MIS). For example, the designation n^{++} Si(100)/poly(MMA-co-ThS)/Al means that the wafer is high-alloyed n^{++} silicon, the layer is the polymer mentioned above, and the top electrode is Al.
[28] J. Jeong, M. J. Kim, W. S. Hwang, B. J. Cho, *Adv. Electr. Mater.* **2021**, *7*, 2100375.
[29] B.-H. Lee, H. Bae, H. Seong, D. I. Lee, H. Park, Y. J. Choi, S. Im, S. Kim, Y.-K. Choi, *ACS Nano* **2015**, *9*, 7306.
[30] I. K. Shundrina, D. S. Odintsov, I. A. Os'kina, I. G. Irtegova, L. A. Shundrin, *Eur. J. Org. Chem.* **2018**, *26*, 3471.
[31] D. S. Odintsov, I. K. Shundrina, I. A. Os'kina, I. V. Oleynik, J. Beckmann, L. A. Shundrin, *Polym. Chem.* **2020**, *11*, 2243.
[32] V. N. Kruchinin, D. S. Odintsov, L. A. Shundrin, I. K. Shundrina, S. V. Rykhlitsky, E. V. Spesivtsev, V. A. Gritsenko, *Opt. Spectr.* **2022**, *130*, 2114.

[33] D. S. Odintsov, I. K. Shundrina, A. A. Gismatulin, I. A. Azarov, R. V. Andreev, V. A. Gritsenko, L. A. Shundrin, *J. Struct. Chem.* **2022**, *63*, 1811.
[34] Z. M. Elimat, A. M. Zihlif, M. Avella, *J. Exp. Nanosci.* **2008**, *3*, 259.
[35] E. V. Spesivtsev, S. V. Rykhlitskii, V. A. Shvets, *Optoelectron. Instrum. Data Process.* **2011**, *47*, 419.
[36] M. V. Zamoryanskaya, S. G. Konnikov, A. N. Zamoryanskii, *Instrum. Exp. Tech.* **2004**, *47*, 477.
[37] N. V. Vasilieva, I. G. Irtegova, V. A. Loskutov, L. A. Shundrin, *Mendeleev Commun.* **2013**, *23*, 334.
[38] D. S. Odintsov, I. K. Shundrina, D. E. Gorbunov, N. P. Gritsan, J. Beckmann, L. A. Shundrin, *Phys. Chem. Chem. Phys.* **2021**, *23*, 26940.
[39] Y. N. Novikov, V. A. Gritsenko, *J. Non-Cryst. Solids* **2022**, *582*, 121442.
[40] S. Makram-Ebeid, P. Boher, M. Lannoo, *Appl. Phys. Lett.* **1987**, *50*, 270.
[41] V. N. Abakumov, V. I. Perel, I. N. Yassievich, *Nonradiative Recombination in Semiconductors* (Eds.: V. N. Abakumov, V. I. Perel) Elsevier Science Publishers, BV, Amsterdam **1991**, 320.
[42] S. Makram-Ebeid, M. Lannoo, *Phys. Rev. B* **1982**, *25*, 6406.
[43] K. A. Nasyrov, V. A. Gritsenko, *J. Appl. Phys.* **2011**, *109*, 093705.
[44] T. V. Perevalov, A. A. Gismatulin, D. S. Seregin, Y. Wang, H. Xu, V. N. Kruchinin, E. V. Spesivcev, V. A. Gritsenko, K. A. Nasyrov, I. P. Prosvirin, J. Zhang, K. A. Vorotilov, M. R. Baklanov, *J. Appl. Phys.* **2020**, *127*, 195105.
[45] Solvation has a minimal effect on the maxima positions of the optical absorption bands of electrochemically reduced polymer films with pendant groups in the polymer structure compared to the spectra of its reduced solution or the electrochemically reduced solution of pendant group precursors.[29,36].
[46] M. A. Lampert, P. Mark, *Current Injection in Solids*, Academic Press, New York **1970**.
[47] A. A. Gismatulin, G. N. Kamaev, V. N. Kruchinin, V. A. Gritsenko, O. M. Orlov, *Sci. Rep.* **2021**, *11*, 2417.
[48] R. D. Duling, *J. Magn. Reson.* **1994**, *104*, 105–110.
[49] V. G. Polovinkin, *Thin Solid Films* **2004**, *455*, 101.
[50] S. Tsuda, S. Yamaguchi, Y. Kanamori, H. Yugami, *Opt. Express* **2018**, *26*, 6899.
[51] H. Hu, R. G. Larson, *J. Phys. Chem. B* **2002**, *106*, 1334.

Manuscript received: March 11, 2024
Revised manuscript received: June 18, 2024
Accepted manuscript online: June 28, 2024
Version of record online: ■■, ■■

RESEARCH ARTICLE

A methyl methacrylate copolymer containing electron-withdrawing 9H-thioxanthen-9-one pendant groups in its structure (poly(MMA-co-ThS)) was synthesized by radical polymerization. Using temperature measurements of the current–voltage characteristics of the p-Si(100)/poly(MMA-co-ThS)/Al model memory device, it was shown that the charge transport in the copolymer film is well described by the Nasyrov–Gritsenko model of phonon-assisted tunneling between traps. For the first time, the nature of the electron traps as thioxanthenone pendant groups was identified using a combination of spectroelectrochemical and electrophysical measurements.

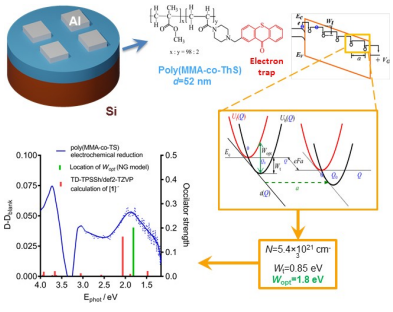

Dr. D. S. Odintsov, Dr. A. A. Gismatulin, Dr. I. K. Shundrina, Dr. A. D. Buktoyarova, Dr. I. A. Os'kina, Prof. Dr. J. Beckmann, Dr. I. A. Azarov, Dr. E. V. Dementeva, Prof. Dr. L. A. Shundrin*, Prof. Dr. V. A. Gritsenko*

1 – 11

Methyl Methacrylate Copolymer with Pendant Thioxanthenone Groups as Active Layer for Resistive Memory Devices